ACP
AMERICAN COLLEGE OF PROSTHODONTISTS®

Confocal Examination of Subsurface Cracking in Ceramic Materials

Maged K. Etman, DDS, MSc, MMedSc, PhD

Division of Prosthodontics, College of Dentistry, University of Saskatchewan, Saskatoon, Canada

Keywords
Ceramics; confocal microscopy; surface cracks; subsurface cracks.

Correspondence
Maged Etman, College of Dentistry, University of Saskatchewan, Division of Prosthodontics, 209 Dental Clinic Bldg., 105 Wiggins Rd., Saskatoon Saskatchewan S7N 5E4, Canada. E-mail: maged.etman@usask.ca

Accepted September 9, 2008

doi: 10.1111/j.1532-849X.2009.00447.x

Abstract

Purpose: The original ceramic surface finish and its microstructure may have an effect on crack propagation. The purpose of this study was to investigate the relation between crack propagation and ceramic microstructure following cyclic fatigue loading, and to qualitatively evaluate and quantitatively measure the surface and subsurface crack depths of three types of ceramic restorations with different microstructures using a Confocal Laser Scanning Microscope (CLSM) and Scanning Electron Microscope (SEM).

Materials and Methods: Twenty ($8 \times 4 \times 2$ mm^3) blocks of AllCeram (AC), experimental ceramic (EC, IPS e.max Press), and Sensation SL (SSL) were prepared, ten glazed and ten polished of each material. Sixty antagonist enamel specimens were made from the labial surfaces of permanent incisors. The ceramic abraders were attached to a wear machine, so that each enamel specimen presented at 45 degrees to the vertical movement of the abraders, and immersed in artificial saliva. Wear was induced for 80K cycles at 60 cycles/min with a load of 40 N and 2-mm horizontal deflection. The specimens were examined for cracks at baseline, 5K, 10K, 20K, 40K, and 80K cycles.

Results: Twenty- to 30-μm deep subsurface cracking appeared in SSL, with 8 to 10 μm in AC, and 7 μm close to the margin of the wear facets in glazed EC after 5K cycles. The EC showed no cracks with increasing wear cycles. Seventy-μm deep subsurface cracks were detected in SSL and 45 μm in AC after 80K cycles. Statistically, there was significant difference among the three materials ($p < 0.05$). Bonferroni multiple comparison of means test confirmed the ANOVA test and showed that there was no statistical difference ($p > 0.05$) in crack depth within the same ceramic material with different surface finishes.

Conclusions: The ceramic materials with different microstructures showed different patterns of subsurface cracking.

Laboratory load failure tests attempt to simulate clinical failure to investigate variables thought to influence the success of dental materials and to evaluate new materials or designs. These tests involve loading a surface of a material with a spherical indenter or equivalently using a flat compression pattern against a curved incisal edge.[1,2] Little attention has been paid to the stress state at failure, or to the mechanism by which failures occur during testing, especially crack initiation and propagation before complete fracture.

Dental restorations are subject to intermittent forces during mastication with maximal occlusal forces that range from 200 to 1000 N.[3] When forces of this magnitude are applied to a small surface area, as during tooth-material contact, substantial stresses are generated, and each stress is capable of creating a corresponding deformation or strain in the contacting bodies. Brittle dental ceramics are incapable of absorbing appreciable amounts of elastic strain energy before fracturing.[4,5] The resistance of a material to crack propagation is one measure of the strain-energy-absorbing ability of a brittle material;[6] it also depends on the composition of the ceramic.[7] It was reported that the fracture toughness values of most dental ceramics examined were slightly higher than that of soda lime glass, but less than one-third that of zirconia.[7]

Fracture toughness of IPS e.max Press was measured with different methods, and it was found that values measured largely depend on the measuring method used.[8,9,10]

The techniques of assessing the resistance of brittle materials to crack initiation and propagation depend on direct measurement of surface radial crack length, which is visible to the naked eye and does show microcrack initiation and propagation

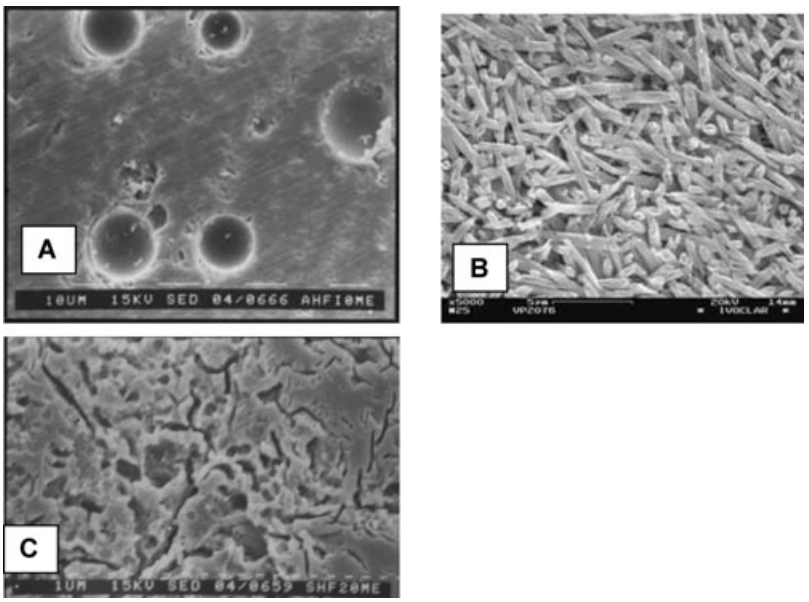

Figure 1 SEM photomicrographs: (A) Rounded structure in homogeneous glassy matrix in AllCeram. (B) Densely packed rod-like crystals of lithium disilicate crystals in experimental glass-ceramic (Courtesy of Ivoclar-Vivadent); from a pilot study. (C) Leucite glass ceramic in Sensation SL.

before fracture.[6,11] It does not measure the depth of the subsurface cracking in relation to the microstructure of a material. Often the test does not simulate the stress applied to the restoration clinically. The relevance of cone cracks in ceramic restoration failures has been questioned.[12] Previous studies report the use of SEM and optical examination using a stereobinocular microscope to determine subsurface cracks in ceramics.[13,14] There have been no reports quantitatively measuring the subsurface cracks in ceramic restorations.

This study tested the null hypothesis that the microstructure and surface finish of all-ceramic restorations have an effect on the magnitude of subsurface crack formation and propagation and can be measured quantitatively.

Materials and methods

Three types of ceramic materials with different microstructures (Fig 1) were used in this study (Table 1). Twenty ($8 \times 4 \times 3$ mm^3) cusp-shaped specimens of ceramic, ten glazed and ten polished of each material, were fabricated following the manufacturer's instructions. For the glazed group, the thickness of the glaze layer was in the average of 30 to 50 μm, confirmed using an UltraVIEW Confocal Laser Imaging Microscopy System (CLSM, Perkin Elmer, Salem, MA). All specimens in the polished group were polished using a series of polishing systems down to 2 μm particle size.[15,16] Sixty antagonist enamel specimens were made from the labial surfaces of permanent incisors. The specimens were attached to a specially designed wear machine.

Table 1 Ceramic materials used

Trade name	Composition	Manufacturer
AllCeram	AllCeram (feldspathic low-fusing porcelain)	Ducera Dental GmbH & Co. KG, Rosbach, Germany
Sensation SL	Glass-ceramic, Leucite-reinforced glass-ceramic	Leach & Dillon Products, Cranston, RI
IPS e.max Press Experimental glass ceramic	Glass-ceramic, densely packed rod-like lithium disilicate crystals	Ivoclar, Schaan, Liechtenstein

Wear machine

The wear testing machine (Fig 2) comprised six cylindrical plungers, which were connected from one side to six identical sample chambers. The cylindrical plungers were connected from the other side to rocker arms. These in turn were in contact with eccentric cams driven by an electric motor. This motor allowed a horizontal sliding motion of the samples so that the plungers produced a vertical reciprocating movement of 2 mm at maximum speed of 60 strokes per minute against the antagonistic specimens in each sample chamber. The wear machine was designed to achieve the following experimental objectives:

1) To produce wear by sliding enamel or ceramic specimens against opposing enamel specimens. The enamel (control group) and the ceramic specimens were attached to the plunger arms (maxillary components), and the enamel specimens (mandibular component) were presented at a 45 degrees angle to the vertical movement of the maxillary component, which held the ceramic and enamel specimens. This was designed to simulate the masticatory movements so that an element of fatigue is superimposed upon sliding wear. A brass hinge mechanism with an attached spring was designed as part of a permanent attachment to the plunger arm, enabling lateral displacement of tooth specimens as they contacted and slid across the material specimens. The function of the spring was to provide a

given load during this lateral displacement and to reposition the tooth specimens during the upward stroke of the plunger (Fig 2).
2) The enamel (control group/maxillary component) and ceramic specimens had to be mounted on the plungers in such a way that they could be removed, measured, and remounted in the same position. This required the design and construction of brass tooth specimen holders, which could be fitted onto the permanent brass plunger attachments. A square fitting was designed with the male component attached to the plunger and the female component being part of the tooth specimen holder. This geometrical design prevented any unwanted rotational movement of the tooth specimens and allowed for accurate repositioning.
3) The enamel specimens (mandibular component) were embedded in brass specimen holders, and these in turn were securely positioned at 45 degrees to the horizontal plane in clear Perspex containers, which were fitted onto the machine. The square fitting was chosen to prevent rotational movement of the material specimens.

A pilot study was carried out to test the feasibility of the design and to establish the required load and cycling period necessary to produce a measurable amount of wear. Phosphor Bronze springs of various thicknesses were tested, and springs of 0.5 mm thickness providing a 40 N load per 2 mm of lateral deflection were chosen.

Test material specimens

Twenty specimens of each ceramic material were prepared according to the manufacturer's instructions. Ten were glazed and ten were polished. All specimens were screened for cracks or surface defects using the CLSM. All specimens that showed cracks or surface defects were discarded and replaced. Ten tooth enamel specimens were used as a control group. The test specimens were rectangular with one rounded corner. This rounded part of the rectangle was abraded against the tooth enamel specimen (abrader). The measurements of the test specimen were: x = 8 mm; y = 4 mm; and z = 3 mm. The curved configuration was selected for the following reasons:

1) To examine the antagonistic enamel wear with a standardized cusp configuration.
2) The shape of the abrader was important. A cylindrical or flat abrader has the disadvantage that edge loading tends to plough the surface of the specimen, thus accelerating wear and altering the mechanism of wear. A curved (spherical) abrader avoided such problems.
3) The control group was enamel cusp tip to flat surface enamel; the cusp tip of the tooth was curved.
4) With curved surfaces, it was possible to visualize the contact point between the two surfaces.

Mounting of the test material specimens

Six cylindrical brass specimen holders (Fig 2) were designed and constructed to ensure tooth and material specimens could be easily removed and replaced in the machine in exactly the same position. A slot was made in one side of the specimen holders for placement of the test materials and tooth pieces. This measured 12 mm in length, 5 mm in width, and 2 mm in depth. A square cavity with dimensions of $10 \times 10 \times 6$ mm^3 was prepared on the opposite side, which enabled the specimen holders to be mounted to matching square fixtures attached to the plungers of the wear machine. Square fittings enabled accurate repositioning and prevented rotational movement of the specimen holders. The specimen holders were secured into position with the aid of an anterior screw.

Each material specimen (AllCeram, Sensation SL, Experimental ceramic, and tooth enamel as a control group) was secured in a cylindrical brass specimen holder. Twenty specimens from each ceramic material group (ten glazed and ten polished) and ten enamel specimens were prepared and placed in the brass specimen holders making a total of 70 specimens. Ceramic materials and tooth enamel specimens were accurately positioned in the specimen holders so presentation of the enamel surface to the opposing enamel abrader surface could be standardized. This was accomplished by means of a brass-mounting jig. Each specimen holder was seated onto a square block on the mounting jig. The specimens could then be placed in uncured composite resin in the prepared slot of the specimen holder. The height, position, and inclination of the tooth piece were gauged by means of a brass-positioning arm on the jig. Once in position the resin composite was light-cured for 40 seconds. Further incremental packing was carried out to secure the tooth piece. In total, six specimen holders were mounted on the machine at any one time. After completion of testing and following crack measurement, the tooth and material specimens were removed from the brass holders with high-speed diamond fissure burs using an air-turbine hand piece. These were then discarded and new specimens mounted.

Test methods

A wear machine[17] was used in this study to simulate the clinical fatigue loading of the three different ceramic materials (abraders) opposing enamel. The abraders were attached to the wear machine and immersed in artificial saliva so each enamel specimen presented at 45° to its vertical movement. The cusp-shaped ceramic specimens slid across the enamel surface with a 2 mm linear path, delivering a 40 N load with a maximum speed of 60 strokes per minute, thus generating wear tracks. This sequence was repeated for 5K, 10K, 20K, 40K, and 80K cycles. The specimens were removed after each sequence, cleaned in the ultrasonic bath with distilled water for 10 minutes and dried with compressed air. Cracks were measured using a Confocal Laser Scanning Microscope (CLSM) and SEM, and the specimens were repositioned on the machine.

Quantitative measurement of depth of cracks

Cracks were measured using CLSM with ×60/1.4 numerical aperture (NA) and ×100/1.3 NA oil lens after application of fluorescence wetting solution. Rhodamine B (Sigma Chemical Co. St. Louis, MO) dissolved in a silane coupling agent as a wetting solution (Monobond-S, Ivoclar-Vivadent, Schaan, Liechtenstein) was applied using a microbrush to highlight cracks and defects. The location of the potential wear tracks was located at baseline by selecting the point of maximum radial convexity when the ceramic surface was at 90 degrees to the optical axis

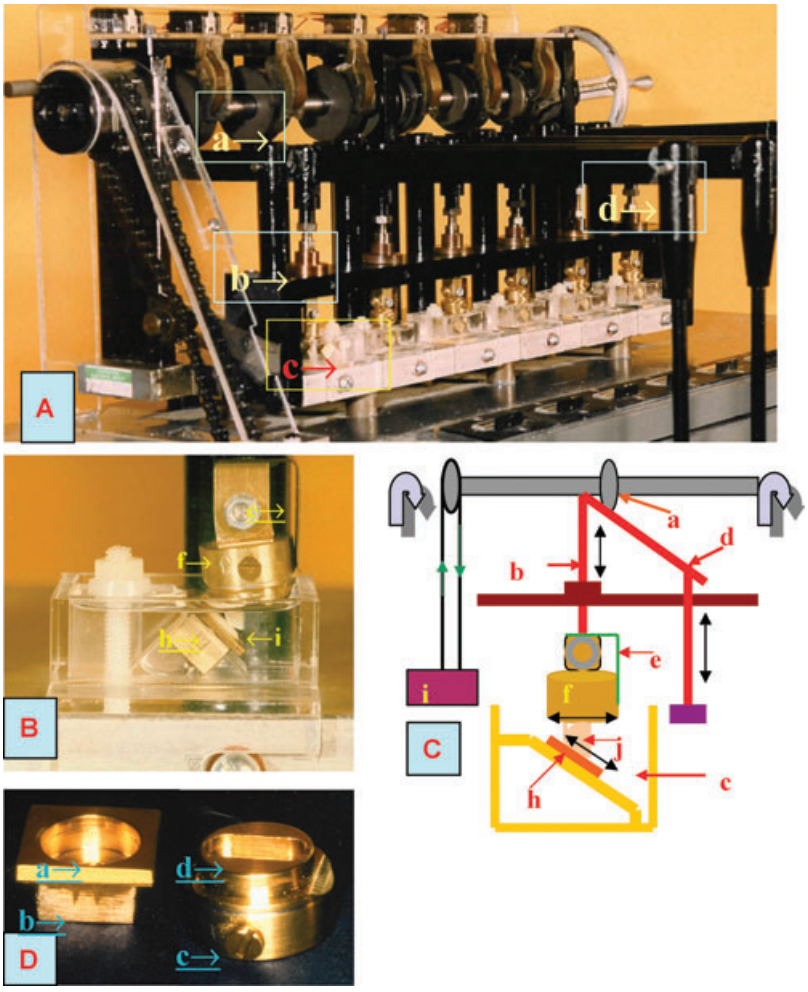

Figure 2 Wear machine components and specimen alignment. Wear machine (A, C): (a) eccentric cams, (b) cylindrical plungers attached to sample (maxillary component), (c) clear Perspex containers with the aligned specimens, and (d) rocker arms in contact with eccentric cams. (B, C): Clear perspex container with the aligned specimens: (e) phosphor bronze spring, (f) specimen holder (test material), (j) test material, (h) specimen holder (enamel abrader), and (i) motor. (D) Enamel brass sample holder (a) mandibular component, which has a cylindrical recess (10-mm diameter, 4-mm depth) prepared for placement of the enamel abrader, (b) square-fitting side, (c) brass tooth/enamel specimen holders, and (d) the prepared recess in the brass specimen holders to accommodate the test material specimens, which could be fitted onto the permanent brass plunger attachments.

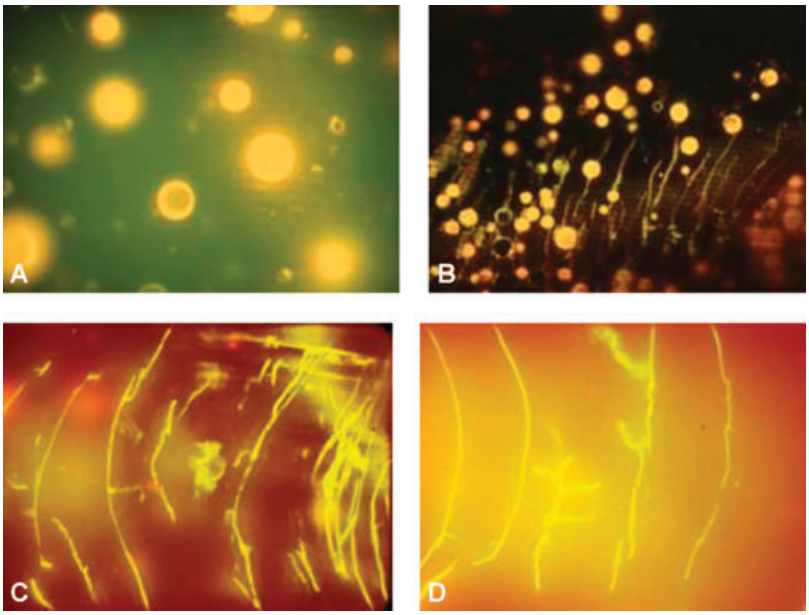

Figure 3 CLSM images of subsurface cracks in AllCeram: (A) Baseline 5 μm below the surface; (B) 5-μm subsurface, note the rounded features and the crack lines; (C) 8–10 μm below the surface, spherical features may be porosity or microstructures; the cracks show up clearly using CLSM in this combined image; and (D) The same field of view, 25 μm below the surface. Perkin-Elmer LSR Ultrview CLSM, $\times$100/1.3 Oil (A, C, D; 102 μm); $\times$20/0.80 Oil (B; 430 μm).

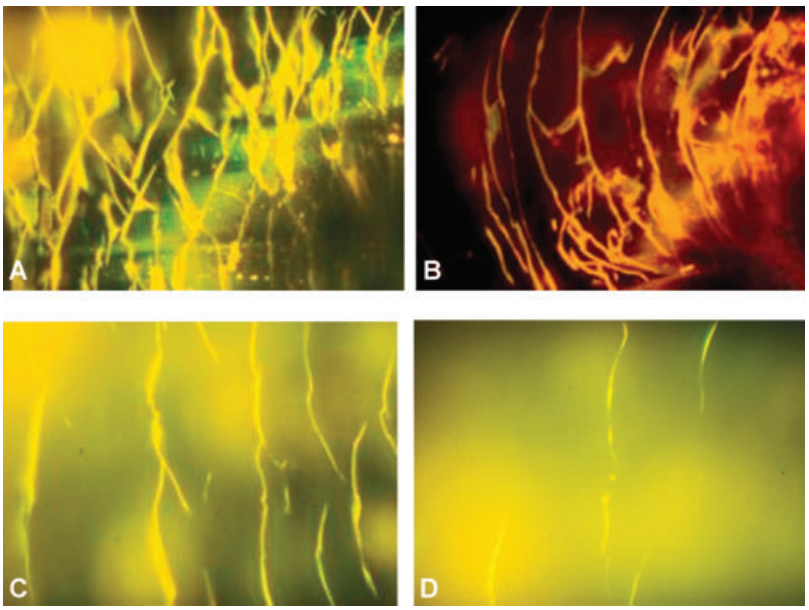

Figure 4 CLSM images of surface and subsurface cracks in Sensation SL: (A) Just below the surface, this was a polished surface of Sensation SL; large number of cracks is very apparent. (B) Sensation SL near the surface, cracks at 90 degrees to the wear cracks. (C) The same sample in (D) 20 μm below the surface, the cracks are broadly parallel and at 90 degrees to the wear tracks. (D) The same field of view, 60 μm below the surface. Perkin-Elmer LSR Ultrview CLSM, ×100/1.3 Oil. Field width 102 μm.

of the confocal microscope. The surface and subsurface regions of the worn ceramics were evaluated, and crack depth was measured at four points on the wear facet. Photomicrographs were taken. SPSS statistical software (SPSS, version 15, SPSS Inc., Chicago, IL) was used for data analysis. The data were analyzed using ANOVA and a variety of general linear modeling statistical tests.

Qualitative measurement of depth of cracks

SEM was used for the qualitative evaluation of surface cracks of the ceramic materials using replicas and the actual ceramic specimens. Replicas were made at baseline, 5000, 10,000, 20,000, 40,000, and 80,000 cycles using poly(vinyl siloxane) elastomeric impression material (President, Coltene Inc. Altstatten, Switzerland) following a standardized impression technique. After 80,000 cycles, the ceramic specimens were cleaned in the ultrasonic bath (Model T14, L & R Mfg., Kearny, NJ) with distilled water for 10 minutes, and then dried with compressed air. The replicas and the actual ceramic specimens were gold sputter-coated for SEM (Model S 520, Hitachi, Tokyo, Japan) examination, and photomicrographs were recorded.

Results

CLSM examination revealed different microstructures and crack patterns in each material. AllCeram specimens revealed

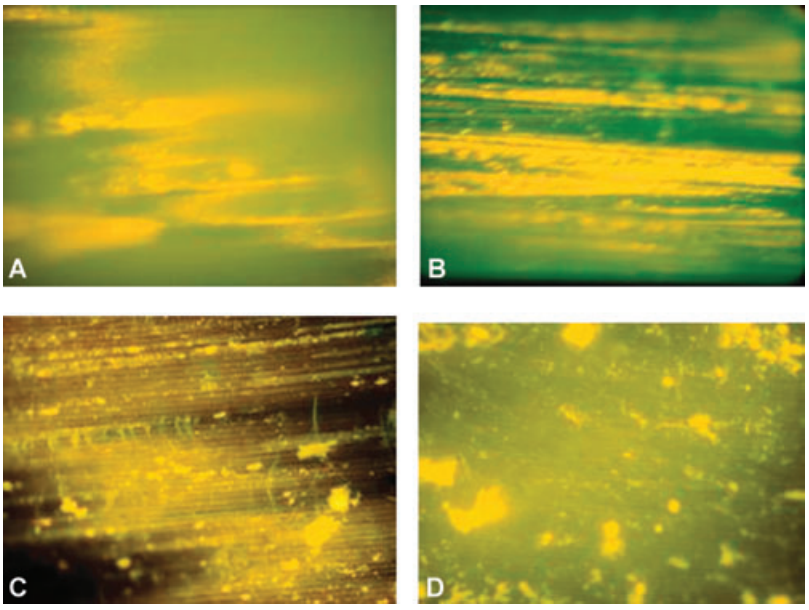

Figure 5 CLSM image of cracks in experimental ceramic: (A) 10-μm subsurface view of glazed surface near the margin of a wear facet; note the disappearance of subsurface cracks. (B) Experimental ceramic, view of the polished surface; note the absence of cracks (C) surface view of glazed surface near the margin of a wear facet, cracks at 90 degrees to the wear tracks. (D) The same sample in (C), 7-μm subsurface view; note the disappearance of subsurface cracks. Perkin-Elmer LSR Ultrview CLSM, ×60/1.4NA Oil. Field width 170 μm.

a uniform distribution of large granular or spherical structures with an average 5-μm size in a homogenous background (Fig 3A). Intergranular and transgranular subsurface cracks were visible (Fig 3B). Sensation SL showed signs of subsurface cracks in a crystalline glassy matrix and a less granular structure than AllCeram. The cracks were parallel to each other and perpendicular to the direction of the wear tracks (Fig 4A). The worn surfaces of the experimental ceramic specimens displayed homogeneous structures with no signs of subsurface cracks in the polished specimens (Fig 5A, B). The glazed group showed up to 7 μm subsurface cracks near the outer surface of the wear facets (Fig 5C, D). These cracks were multiple and confined only to the glaze layer. Subsurface imaging showed little evidence of porosity in this material. Sensation SL showed a range of 20- to 30-μm deep subsurface cracking (Fig 4C), while 8- to 10-μm deep cracks were apparent in AllCeram after 5000 cycles (Fig 3C). The surface cracking of the glazed groups in both ceramics showed multiple cracks propagating in different directions. The subsurface cracks were continuous and not branched. The depth of the subsurface cracks increased with greater number of fatigue loading cycles in both AllCeram (Fig 3D) and Sensation SL (Fig 4D). The experimental ceramic showed no cracks with increasing wear cycles. Up to 70-μm deep subsurface cracks were detected after 80K cycles in Sensation SL, while AllCeram showed a 45-μm maximum depth of crack. Table 2 shows the means and standard deviations of crack depths at different number of cycles. Statistically, ANOVA revealed a significant statistical difference in crack depth between the three types of ceramic materials ($p < 0.05$). Bonferroni Multiple Comparison of Means test confirmed the ANOVA test and showed that there was no statistical difference ($p > 0.05$) in crack depth within the same ceramic material with different surface finishes. Figures 6 and 7 show the change in the depth of cracks for each ceramic system at different numbers of wear cycles.

Table 2 Means and standard deviations (SD) of crack depth

	Crack depth (micron)				
	Wear cycles				
Ceramic material	5000	10,000	20,000	40,000	80,000
AllCeram polished					
Mean	8.55	10.07	15.40	23.88	32.15
SD	1.961	2.654	4.290	3.031	7.850
AllCeram glazed					
Mean	8.45	13.40	18.05	24.45	33.98
SD	1.739	2.479	3.782	6.441	10.060
Sensation SL polished					
Mean	12.43	18.88	24.65	30.13	39.40
SD	4.057	4.863	4.995	8.582	10.507
Sensation SL glazed					
Mean	11.70	14.70	25.55	32.53	42.88
SD	2.738	4.109	5.104	6.887	8.386
Experimental polished					
Mean	0.25	0.00	0.00	0.00	0.00
SD	0.954	0.000	0.000	0.000	0.000
Experimental glazed					
Mean	3.73	0.72	0.58	0.70	0.10
SD	4.076	1.783	1.647	1.636	0.632

Qualitative surface crack measurement

SEM showed that the microcracks' shape, distribution, and location were different from one material to another. The microcracks in Sensation SL were related to the wear facets and perpendicular to the wear tracks. Cracks in this material were semicircular and were distributed all over the wear facets (Fig 8). This material showed a uniform distribution of crack lines with no evidence of microcracking in the semicircular crack patterns.

AllCeram was quite different in that there was much more chipping and bulk fracture of the materials (Fig 9). The fracture followed the direction of the sliding force and was represented by wear tracks. The experimental ceramic showed no cracks on the worn surfaces (Fig 10A). The margin of the wear facets showed the remnants of the glaze material with fine cracks (Fig 10B).

Discussion

The results of this study showed that the experimental glass-ceramic with its unique microstructures was more crack resistant than other ceramic materials.

When grinding forces were measured in alumina and glass-ceramics with various microstructures, it was found that the microstructures exerted a profound influence on machinability. In particular, the controlling toughness variable is that which pertains to small cracks, not that conventionally measured in a large-scale fracture specimen.[18] In a clinical study, Etman et al[19] reported that the IPS e.max Press ceramic material showed a friendly wear behavior on the opposing tooth enamel and yet was more wear resistant than the Procera AllCeram system. Another study reported that the three all-ceramic materials caused enamel wear and were worn by enamel; none retained final surface finish. The mean depth of wear of the test materials were: AllCeram (polished, 254.17 μm; glazed, 264.48 μm), Sensation SL (polished, 268.09 μm; glazed, 265.69 μm), experimental ceramic (polished, 196.90 μm; glazed, 201.62 μm), and tooth enamel (184.48 μm). The antagonists' tooth enamel showed wear caused by the four test materials. The mean depth of wear in the enamel antagonists were 248.04 μm and 260.34 μm caused by AllCeram polished and glazed, respectively. Sensation SL caused enamel wear (polished, 270.04 μm; glazed, 264.05 μm). The experimental ceramic caused less wear than the other two all-ceramic materials but more wear than tooth enamel. The polished experimental ceramic caused a 197.90-μm depth of wear, while the glazed specimens caused a 201.30-μm mean depth of wear. Tooth enamel caused wear for the opposing tooth enamel with mean depth of wear 178.36 μm. This may confirm the relation between microstructures, microcracks, and wear behavior.[20]

In recent years, many ceramic materials have been developed with different proportions of glassy and crystalline phases aiming to improve their physical and mechanical properties. Different phases in these multiphase ceramic materials may react in a different way to cyclic fatigue loading and may have an effect

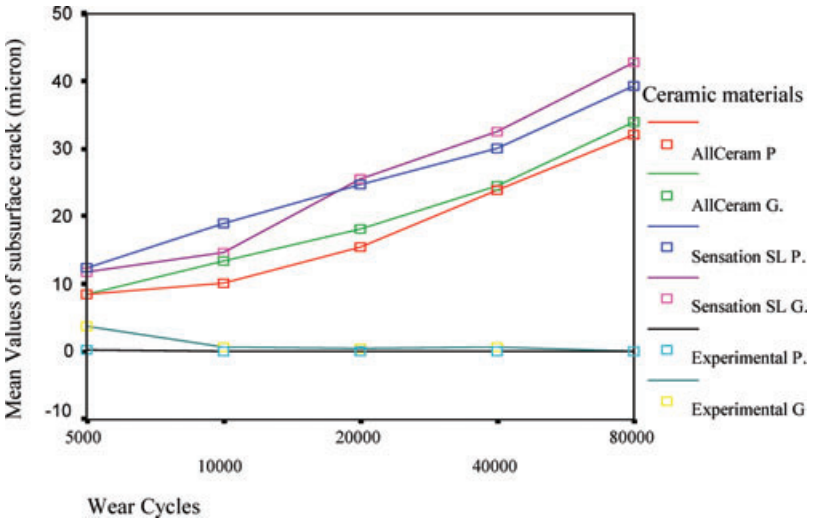

Figure 6 Mean values of crack depth over different groups of wear cycles.

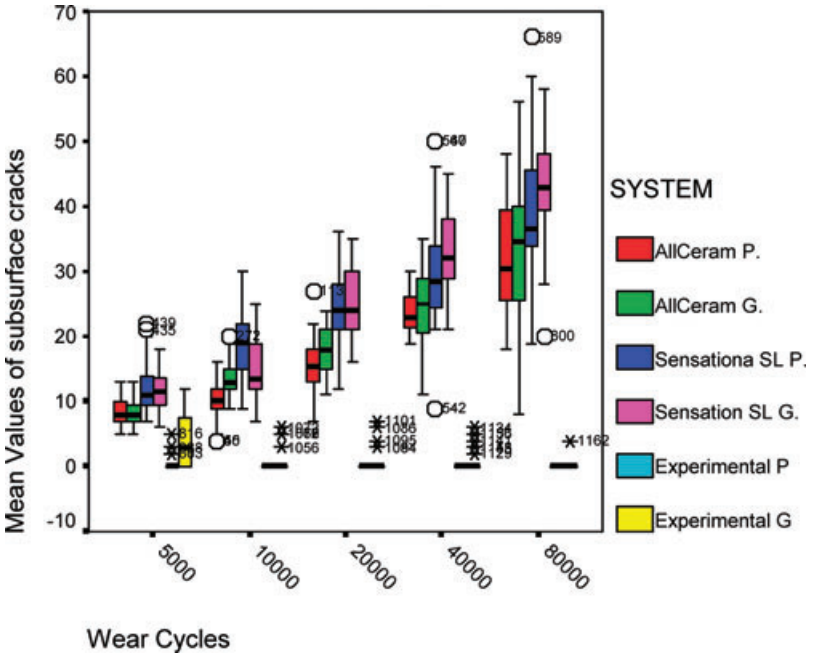

Figure 7 Box plot shows medium distribution, 75% and 25% of each distribution and extreme values at different wear cycles.

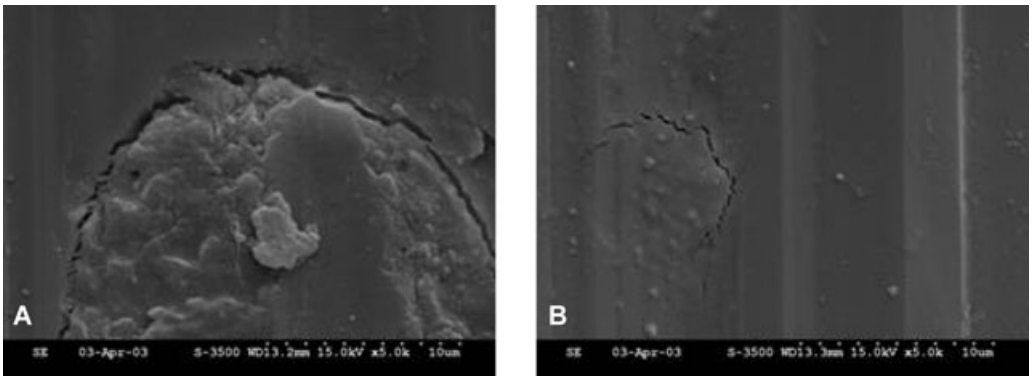

Figure 8 SEM photomicrographs of the worn Sensation SL ceramic show circular crack lines in both glazed (A) and polished (B) worn surfaces after 80,000 wear cycles. (Original magnification ×5000).

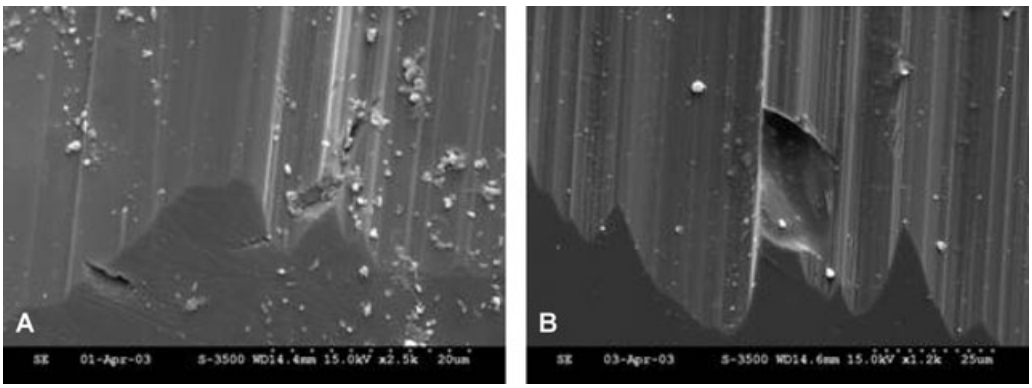

Figure 9 SEM photomicrographs show bulk fracture of AllCeram in both polished (A) and glazed (B) samples after 80,000 wear cycles. Original magnification, ×2500 (A); ×1200 (B).

on crack initiation and propagation. In this study, surface and subsurface cracks were investigated, with the results revealing that surface and subsurface cracks were dependent on the type of ceramic material.

The experimental hot-pressed lithium disilicate glass-ceramic material showed the highest resistance to crack formation and propagation. This may be due to the crystalline phases in this material. It has been reported that the crystalline phases in ceramic materials may act as crack stoppers to prevent crack propagation;[21] however, with Sensation SL, this was not the case in this study. The high leucite crystalline structure showed the least resistance to crack propagation. This may be attributed to phase interaction and separation. The promotion of interaction between fatigue crack and microstructure**,** such as microcracking and phase transformation and separation in the process zone, has been reported.[22] AllCeram showed less crack propagation than Sensation SL, even though it is single phase low-fusing feldspathic porcelain. Crack initiation and propagation in this material may be explained by correlation between microcracks, porosity, and microstructures. It has been reported that the equilibrium between the external and internal forces inside the damage zone correlates with microstructural features, such as grain size distribution.[23] Crack propagation may depend on the compatibility between the phases in each material and some other microstructural factors, such as density of the material and porosity.

In the first 5000 cycles, AllCeram, Sensation SL, and the experimental ceramic showed multiple crack lines on the glazed surface. With an increasing number of wear cycles, the glaze layer was removed from the surface of the experimental ceramic leaving a crack-free surface. On the other hand, Sensation SL developed more cracks that propagated deeper into the material once the glaze layer was worn away. This may be explained as the driving force required for crack propagation being supplied continuously by the external stress-caused phase separation at a low energy level. These external stresses can provide sufficient energy for crack formation, especially as the crack becomes larger at constant load.[24] Upon loading the material and inducing stresses, phase separation may occur. This would explain the irregular pattern of cracks in some specimens of this material, which are similar to the shape and distribution of the leucite phase; however, another study reported that the crystalline inclusion was thought to help blunt fracture progression and improve fracture resistance.[25] Another possible cause of Sensation SL cracks might be thermal mismatch between the leucite phase and the glassy matrix. Also the inclusion of

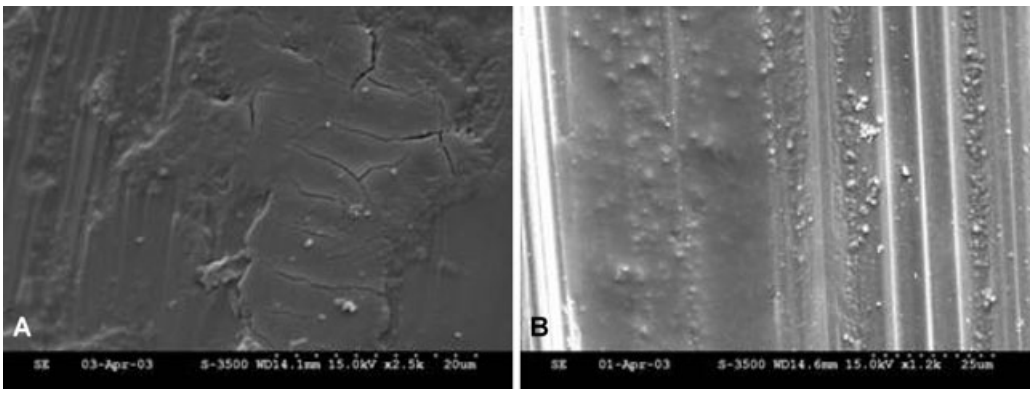

Figure 10 SEM photomicrographs of the worn experimental ceramic show crack lines located in the glaze layer at 90 degrees to the wear tracks (A); note, no cracks in the polished worn surface after 80,000 wear cycles. Original magnification, ×2500 (A); ×1200 (B).

large particle sizes of crystalline phases into a glassy matrix may have a direct correlation to crack formation.[26,27] A smaller crystal size could be beneficial to the strength properties of the experimental ceramic.

AllCeram is considered a low-fusing feldspathic porcelain. CLSM showed two phases in AllCeram, one a glassy matrix and the other a sparse rounded structure that may represent a crystalline phase or porosity. SEM photomicrgraphs showed pores on the surface. Both AllCeram and Sensation SL were made using a powder and condensing liquid and repeated firing. This method has inherent problems, such as porosity, that may cause internal microcracks and phase separation from the use of physical mixtures of the glass powder.[28] While the inclusion of phases of a different refractive index is believed to be beneficial in terms of light scattering within porcelain,[29] problems may ensue due to incompatibility of thermal expansion of the various phases present.[30,31] Imaging of AllCeram worn surfaces showed a high proportion of spherical-type pores that may cause further cracking. Small cracks around the periphery of a void have been cited as causing failure due to the stress concentration at the void.[32] In this study, the catastrophic effect of cracking is more evident around the larger-sized voids in the AllCeram samples. Pores arresting cracks have been described.[33] The crack awaits a load rise to break away or requires extra energy to curve out of the main crack plane because of the pore-stress field. This theory was based on evenly spaced and sized pores and does not totally equate to the differing pore size and distribution in AllCeram. Nevertheless, there is an obvious crack-pore interaction.

The experimental ceramic is composed mainly of an interlocking pattern of many elongated lithium disilicate crystals (length up to 6 μm, diameter up to 1 μm) and secondary lithium orthophosphate crystals (0.1 to 0.3 μm).[34] Hot-pressing and continuous growth of the dimensions of these crystals upon heating may create a more dense structure. This may explain the crack resistance of this material.

The SEM examination confirmed the CLSM finding, but only on the worn surfaces. This showed the microcracks' shape, distribution, and location are different from one material to another. The microcracks in Sensation SL related to the wear facets and were perpendicular to the wear tracks. Cracks in this material are semicircular and are distributed all over the wear facets. Also, this material showed considerably more uniform distribution of crack lines with evidence of microcracking in the semicircular crack patterns. This crack pattern may be related to the leucite-shaped crystals that form the main component of this material. AllCeram was quite different in that there is much uniform distribution of a small amount of large crystals. Although there are small cracks within the crystals, these do not extend into the glass matrix. There was also evidence of microcracking within the crystals, and in some instances, cracks ran from the glassy matrix into and through the large crystalline structures. These round structures may have stopped crack propagation.

The presence of microcracks around the clusters of leucite crystal may suggest that nonuniform shrinkage of the glassy matrix and crystalline phases had occurred on cooling due to differences in their thermal expansion behavior and the cubic to tetragonal leucite transformation.[30] If this is the case, microcracks would have to be found in the polished surface of these materials, which was not the case. These microcracks can also occur around individual leucite crystals, but only when these are exceptionally large.[31] These microcracks, combined with the nonuniform distribution of the crystalline phase, will severely limit the mechanical properties of these materials, because they increase the inherent flaw size and may act as fracture-initiating flaws,[35] increasing the chances of catastrophic crack propagation. These flaws depend upon the size of the starting particles and distribution of the crystalline phase in the fired ceramics.

Crack formation may serve as a mechanism for relief of the residual stresses.[24] In this manner, the final size of the crack corresponds to the condition of crack arrest. It is speculated that under these conditions the force derived from the relaxation of the residual stress field just suffices to supply the energy required to propagate the crack along a single crack front with little or no probability for secondary cracks or microcrack formation. The deriving force required for crack propagation is supplied continuously by the external stress field, which can provide sufficient energy for microcrack formation, especially as the crack becomes larger at constant load.[24]

The combination of high-strength and fine crystalline structure may have an effect on the long-term performance of all-ceramic restorations, especially in stress-bearing areas. Although no fixed values of masticatory stress could be found in the literature for posterior crowns, using 40 N loads, surface cracks started to develop as early as 5000 wear cycles in the glaze layer. This study showed that these cracks in the glaze layer have no correlation with the underlying ceramic. On the other hand, the subsurface cracks that occurred in the main bulk of the material have a strong correlation with the microstructures of such material.

Conclusions

The microstructure and the technique of build-up of ceramic restorations may have an effect on crack initiation and propagation. An overall view of the data from this investigation suggests that Sensation SL is not much more resistant to crack initiation and propagation than AllCeram. The higher subsurface crack depth of Sensation SL and AllCeram demonstrates the potential unreliability of these materials in stress-bearing areas. High values of subsurface cracks were recorded as early as 5000 loading cycles. The experimental ceramic showed higher resistance to crack formation, and this may make it more reliable for stress-bearing areas. The surface finish has no effect on crack propagation. Knowing the potential for developing cracks in these materials may aid selection in various clinical applications. The CLSM is a useful instrument for detecting subsurface cracks in ceramics.

References

1. Josephson BA, Schulman A, Dunn ZA, et al: A compressive strength study of an all-ceramic crown. J Prosthet Dent 1985;53:301-303
2. Carrier DD, Kelly JR: In-Ceram failure behavior and core-veneer interface quality as influenced by residual infiltration glass. J Prosthodont 1995;4:237-242

3. Waltimo A, Kemppainen P, Kononen M: Maximal contraction force and endurance of human jaw closing muscles in isometric clenching. Scan J Dent Res 1993;101:416-421
4. Wiederhorn SM: Fracture and surface energy of glass. J Am Ceram Soc 1969;52:99-105
5. Doltsinis L, Dattke R: Modelling the damage of porous ceramics under internal pressure. Computer Methods in Applied Mechanics and Engineering 2001;191:29-46
6. Exadaktylos G: Gradient elasticity with surface energy: mode-I crack problem. Int J Solids Struc 1998;35: 421-456
7. Taira M, Nomura Y, Wakasa K, et al: Studies on fracture toughness of dental ceramics. J Oral Rehab 1990;17:551-563
8. Albakry M, Guazzato M, Swain MV: Biaxial flexural strength, elastic moduli, and x-ray diffraction characterization of three pressable all-ceramic materials. J Prosthet Dent 2003;89:374-380
9. Della Bona A, Mecholsky JJ, Anusavice KJ: Fracture behavior of lithia disilicate- and leucite-based ceramics. Dent Mater 2004;20:956-962
10. Guazzato M, Albakry M, Ringer SP, et al: Strength, fracture toughness and microstructure of a selection of all-ceramic materials. Part I. Pressable and alumina glass infiltrated ceramics. Dent Mater 2004;20:441-448
11. Chantikul P, Anstis GR, Lawn BR, et al: A critical evaluation of indentation techniques for measuring fracture toughness: II. Strength method. J Am Ceram Soc 1981;64:539-562
12. Kelly JR: Approaching clinical relevance in failure testing of restorations. J Prosthet Dent 1999;81:652-662
13. Quinn JB, Quinn GD, Kelly JR, et al: Fractographic analysis of three ceramic whole crown restoration failures. Dent Mater 2005;21:920-929
14. Scherrer SS, Quinn JB, Quinn GD, et al: Fractographic ceramic failure analysis using the replica technique. Dent Mater 2007;23:1397-1404
15. Magne P, Oh W, Pintado MR, et al: Wear of enamel and veneering ceramics after laboratory and chairside finishing procedures. J Prosthet Dent 1999;82:669-679
16. Etman MK, Northeast SE, van Noort R: A comparative study of the etched and polished surfaces of two dental and an experimental ceramic. J Dent Res 1999;IADR Abstract No. 1614
17. Etman MK: Clinical and Laboratory Evaluation of Advanced All-Ceramic Restorations. PhD Thesis 2004, University of London
18. Marshall DB, Lawn BR, Cook RF: Microstructural effects on grinding of alumina and glass-ceramics. J Am Ceram Soc 2005;70:139-140
19. Etman MK, Woolford M, Dunne S: Quantitative measurement of tooth and ceramic wear: in vivo study. Int J Prosthodont 2008;21:245-222
20. Etman MK: Wear of experimental ceramic and human enamel: an in-vitro study 2007; (IADR/AADR/CADR, Abstract No. 0183)
21. Shareef MY, Van Noort R, Messer PF, et al: The effect of microstructural features on the biaxial flexural strength of leucite reinforced glass ceramics. J Mater Sci: Materials in Medicine 1994;5:113-118
22. Okabe T, Kido M, Miyahara T: Fatigue fracture behaviour of oxide ceramics in water. Eng Fract Mech 1994;48:137-146
23. Buresch FE: Relations between the damage in and microstructure of ceramics. Mater Sci Eng 1985;71: 187-194
24. Beall GH, Chyung K, Stewart RL: Effect of test method and crack size on the fracture toughness of chain-silicate glass-ceramic. J Mater Sci 1986;21:2365-2372
25. Beham G: IPS empress. A new ceramic technology. ZWR 1991;100:404-408
26. Binns DB: Some physical properties of two-phase crystal glass solids. In Stewart GH (ed): Science of Ceramics, Vol. 1. London, Academic Press, 1962, pp. 315-334
27. Frey WJ, MacKenzie JD: Mechanical properties of selected glass crystal composites. J Mater Sci 1967;2:124-130
28. Piddock V, Marquis PM, Wilson HJ: Structure-property relationships of dental porcelains used in jacket crowns. Br Dent J 1984;156:395-398
29. McLean JW: Aesthetics in restorative dentistry: the challenge for the future. Br Dent J 1980;149:368-374
30. Preston JD (ed): Perspectives in Dental Ceramics: Proceedings of the Fourth International Symposium on Ceramics. Chicago, IL, Quintessence, 1988, p. 53
31. Fairhurst CW, Lockwood PE, Ringle RD, et al: The effect of glaze on porcelain strength. Dent Mater 1992;8:203-207
32. Evans AG, Biswas DS, Fulrath RM: Some effects of cavities on the fracture of ceramic materials: II: spherical cavities. J Am Cerm Soc 1979;62:101-106
33. Nadeau JS, Bennett RC: Some effects of dispersed phases on the fracture behaviour of glass. In Bradt RC, Hasselman DPH, Lang FF (eds): Fracture Mechanics of Ceramics, Vol. IV. New York, Plenum Press, 1978, pp. 961–962
34. Höland W: Materials science fundamentals of the IPS Empress 2 glass-ceramic. Ivoclar-Vivadent Rep 1998;12:3-10
35. Jones DW, Wilson HJ: Some properties of dental ceramics. J Oral Rehabil 1975;2:379